LETTERS

Lanthanide contraction and magnetism in the heavy rare earth elements

I. D. Hughes[1], M. Däne[2], A. Ernst[3], W. Hergert[2], M. Lüders[4], J. Poulter[5], J. B. Staunton[1], A. Svane[6], Z. Szotek[4] & W. M. Temmerman[4]

The heavy rare earth elements crystallize into hexagonally close packed (h.c.p.) structures and share a common outer electronic configuration, differing only in the number of $4f$ electrons they have[1]. These chemically inert $4f$ electrons set up localized magnetic moments, which are coupled via an indirect exchange interaction involving the conduction electrons. This leads to the formation of a wide variety of magnetic structures, the periodicities of which are often incommensurate with the underlying crystal lattice[2]. Such incommensurate ordering is associated with a 'webbed' topology[3,4] of the momentum space surface separating the occupied and unoccupied electron states (the Fermi surface). The shape of this surface—and hence the magnetic structure—for the heavy rare earth elements is known to depend on the ratio of the interplanar spacing c and the interatomic, intraplanar spacing a of the h.c.p. lattice[5]. A theoretical understanding of this problem is, however, far from complete. Here, using gadolinium as a prototype for all the heavy rare earth elements, we generate a unified magnetic phase diagram, which unequivocally links the magnetic structures of the heavy rare earths to their lattice parameters. In addition to verifying the importance of the c/a ratio, we find that the atomic unit cell volume plays a separate, distinct role in determining the magnetic properties: we show that the trend from ferromagnetism to incommensurate ordering as atomic number increases is connected to the concomitant decrease in unit cell volume. This volume decrease occurs because of the so-called lanthanide contraction[6], where the addition of electrons to the poorly shielding $4f$ orbitals leads to an increase in effective nuclear charge and, correspondingly, a decrease in ionic radii.

We report here a theoretical investigation of the onset of magnetic order in the heavy rare earths, focusing on gadolinium as the prototypical member of this series. State-of-the-art computational techniques are used to model the finite-temperature electronic structure of this system, with a completely *ab initio* approach taken and no fitting to experimental parameters. Thermally induced spin fluctuations are treated using a 'local moment' picture of magnetism[7], in which local spin polarization axes are associated with all lattice sites, the orientations of which vary slowly on the timescale of electronic motion. These 'local moment' degrees of freedom produce local magnetic fields on the lattice sites, which affect the electronic motions and are self-consistently maintained by them. By studying the wave vector ($\mathbf{q}$) dependence of the spin fluctuations that characterize the paramagnetic state we gain information about the type of magnetic order that might occur as the temperature is lowered through a phase transition.

For example, in a ferromagnetic material such as gadolinium, the paramagnetic state is characterized by ferromagnetic spin fluctuations that have long wavelengths ($\mathbf{q} \approx 0$) and becomes unstable to these fluctuations at the Curie temperature T_C. For a system that orders into an incommensurate antiferromagnetic structure the paramagnetic state is dominated by 'anti-ferromagnetic' spin fluctuations, specified by a finite, incommensurate, wave vector $\mathbf{q} = \mathbf{Q}_0$ that also characterizes the static magnetization or spin density wave state formed below the Néel temperature T_N. For example, the magnetic structures of the later heavy rare earth elements, terbium to thulium, are described by wave vectors of the form $\mathbf{Q}_0 = \{0, 0, q_{inc}\}$, where individual hexagonal layers are uniformly magnetized in a direction that changes from layer to layer according to the modulation vector q_{inc}. To determine the nature of the spin fluctuations we evaluate the paramagnetic spin susceptibility, $\chi(\mathbf{q}, T)$. This can be written as $\chi(\mathbf{q}, T) = \mu^2/(3k_B T - S^{(2)}(\mathbf{q}, T))$, where μ specifies a local moment magnitude and $S^{(2)}(\mathbf{q}, T)$ mediates the interaction between moments[8]. The wave vector at which $\chi(\mathbf{q}, T)$ and $S^{(2)}(\mathbf{q}, T)$ attain their maxima corresponds to the wave vector of the dominant paramagnetic spin fluctuations.

We started by investigating gadolinium at its equilibrium lattice parameters, both those measured experimentally and also those determined theoretically by minimizing the total energy of the system with respect to changes in the parameters. For a proper description of the electronic structure of gadolinium it was necessary to account for the strong electron–electron correlations of the highly localized $4f$ states. Indeed, on neglecting these strong electron correlations the f-electrons became band-like and we found that at both the experimental and theoretical lattice parameters the system was inclined to order into a commensurate antiferromagnetic structure, with magnetic moments oppositely aligned in alternating planes along the c axis, contrary to the experimentally observed ferromagnetic ordering. Such antiferromagnetic ordering has been found in other conventional electronic structure calculations[9] and is attributed to the presence of minority spin $4f$ electrons at the Fermi energy[10]. To localize the f electrons, previous investigations separated them out from the more itinerant spd electrons, treating them either as part of the core[11] or introducing the effect of strong electron correlations by explicitly including a Coulomb parameter U for the f states[12]. In our investigation we used a different approach, the self-interaction correction technique[13–15] (see Supplementary Methods for details), in which localized and delocalized electrons are treated on an equal footing and the effects of strong Coulomb correlations are incorporated in a parameter-free way.

The picture that emerged from our first-principles theory for $S^{(2)}(\mathbf{q}, T)$, once the f electrons were appropriately localized, was of a magnetic field produced by a $4f$ moment on one atomic site polarizing the conduction electrons. Their induced magnetization then

[1]Department of Physics, University of Warwick, Gibbet Hill Road, Coventry, CV4 7AL, UK. [2]Institut für Physik, Martin-Luther-Universität Halle-Wittenberg, Friedemann-Bach-Platz 6, D-06099 Halle, Germany. [3]Max Planck Institut für Mikrostrukturphysik, Weinberg 2, D-06120 Halle, Germany. [4]Daresbury Laboratory, Daresbury, Warrington, WA4 4AD, UK. [5]Department of Mathematics, Faculty of Science, Mahidol University, Bangkok, 10400, Thailand. [6]Department of Physics and Astronomy, University of Aarhus, DK-8000 Aarhus, Denmark.

interacted with the magnetic fields set up by moments on other sites. Consequently, the moment–moment interaction was governed by the non-interacting susceptibility of the conduction electrons, $\chi_0^{\text{conduction}}(\mathbf{q}, T)$. Such an indirect exchange interaction between moments, mediated by conduction electrons, is referred to as a RKKY (Ruderman–Kittel-Kasuya–Yosida) interaction and experimentally is what drives the magnetism in the heavy rare earth elements[16]. Indeed, with a proper treatment of the f electrons, our calculations predicted a ferromagnetic ground state, in agreement with experiment. The temperature dependency of the susceptibility followed a Curie–Weiss law, with $T_C = 280$ K for the theoretical lattice parameters and 324 K for the experimental lattice parameters. The overestimate of the Curie temperature at the experimental lattice

parameters (experimental $T_C = 293$ K; ref. 2) can be attributed to our mean field treatment of spin fluctuations[17]. The effective magnetic moment was $7.34\mu_B$ for the theoretical lattice parameters and $7.36\mu_B$ for the experimental lattice parameters, in reasonable agreement with the experimental value of $7.63\mu_B$ and also the results of previous studies in which f electrons were treated in a different subsystem to the more itinerant electrons ($7.44\mu_B$ and $7.41\mu_B$; refs 18 and 10, respectively).

The susceptibility of gadolinium for non-equilibrium lattice parameters is shown in Fig. 1. Two variables, the c/a ratio and the unit cell volume, specify the h.c.p. lattice parameters of the heavy rare earth elements. Figure 1a concerns the first. It shows that, for the lowest c/a ratios, gadolinium is no longer predicted to be ferromagnetic, instead adopting an incommensurate magnetic structure. This could be helical, where the helix turn angle, that is, the angle between magnetic moments in adjacent layers, would be given by πq_{inc}, where q_{inc} is the position of the susceptibility peak. Andrianov[19] investigated helical magnetic ordering in several heavy rare earth systems and found the helix turn angle to be a smooth, square-root-shaped function of the c/a ratio. He also noted that it varied by several orders of magnitude while the c/a ratio changed by less than 1%. Such behaviour could possibly be interpreted in terms of an electronic topological transition[20,21] at some critical c/a ratio, where this is a rupturing of the webbing structure found in the Fermi surface of these systems. This webbing structure contains large parallel sheets of Fermi surface, which can 'nest' together when translated by some vector in $\mathbf{k}$-space, and it has been shown, both theoretically[22] and experimentally[23], that the size of this nesting vector is correlated with the magnetic modulation vector.

In our theory, such Fermi surface effects should be contained in $\chi_0^{\text{conduction}}(\mathbf{q}, T)$, because this is determined by excitations from occupied states at all Bloch wave vectors $\mathbf{k}$ to unoccupied states at wave vectors $\mathbf{k} + \mathbf{q}$. $\chi_0^{\text{conduction}}(\mathbf{q}, T)$ is dominated by a Brillouin zone integral[17] $\int A_B(\mathbf{k}, \varepsilon_F) A_B(\mathbf{k} + \mathbf{q}, \varepsilon_F)\, d\mathbf{k}$ where the Bloch spectral function, $A_B(\mathbf{k}, \varepsilon_F)$, gives the density of states at the Fermi energy ε_F at the Bloch wave vector $\mathbf{k}$. It follows that it can develop a peak at a finite Bloch wave vector $\mathbf{q} = \mathbf{Q}_0$ if there are regions of the Fermi surface that coincide when one is translated by a nesting vector $\mathbf{Q}_0$. To analyse the results we obtained in Fig. 1a, we calculated the Fermi surface of paramagnetic gadolinium at various c/a ratios. A 'webbing' structure was indeed found in those systems where incommensurate ordering is predicted (see Supplementary Fig. S1 for three-dimensional illustrations of the Fermi surface), with the nesting vector magnitude coinciding with q_{inc}.

Figure 2 shows cross-sections through the nesting region of the Fermi surface for various c/a ratios. Two extremal nesting vectors, one centred and the other non-centred, were found. The length of the centred nesting vector decreases as the c/a ratio increases, in agreement with the experimental results of Andrianov[19], but contrary to the results in Fig. 1a, where the position of the incommensurate ordering peak is almost invariant to the c/a ratio used. The non-centred vector, however, stays fairly constant as the c/a ratio is altered, indicating this vector to be responsible for the incommensurate ordering observed in our calculations. This agrees with recent theoretical work[24].

We now turn to the magnetic ordering behaviour as a function of unit cell volume. Here we found two distinct cases, dependent on the c/a ratio of the lattice parameters. For high c/a ratios, corresponding to systems with no webbing feature, ferromagnetic ordering was predicted for all volumes. For low c/a ratios, corresponding to systems with webbing, a more complicated picture emerges, as shown in Fig. 1b. The webbing structure leads to an enhancement of the susceptibility at the nesting vector for all volumes. However, for the enhancement to be large enough so that incommensurate ordering wins out over ferromagnetic ordering the unit cell volume needs to be below a certain critical value.
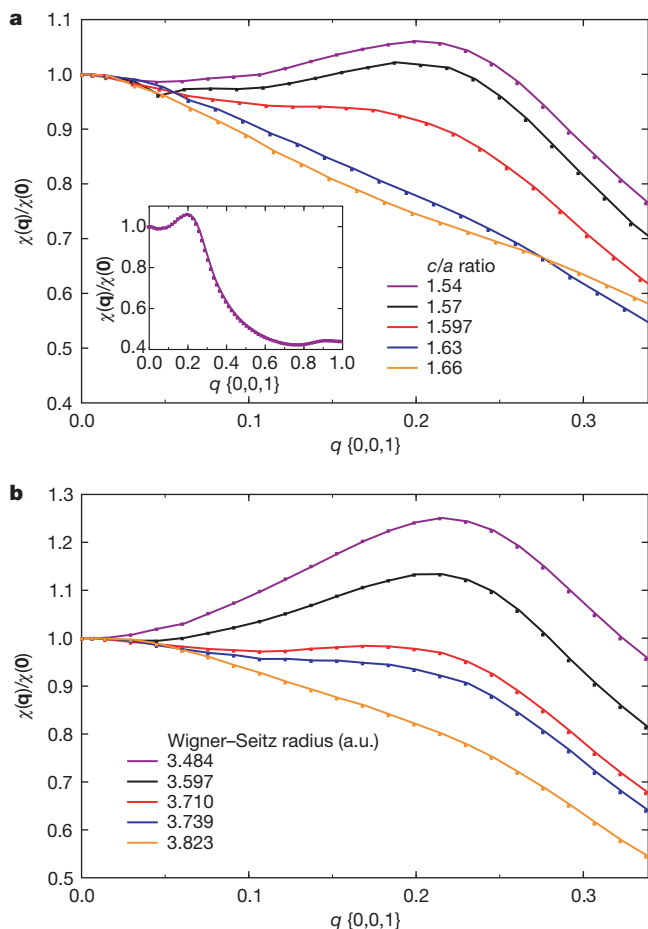

Figure 1 | Normalized paramagnetic spin susceptibilities for gadolinium, obtained from *ab initio* calculations. The data shown is for wave vectors $\mathbf{q}$ along the [0, 0, 1] direction. **a**, Data for various c/a ratios, using theoretical unit cell volumes which were found to be almost invariant to the c/a ratio. The inset shows the susceptibility up to the zone boundary for c/a ratio 1.54. The experimental c/a ratio is 1.597. It is evident that as the c/a ratio decreases, the susceptibility starts to develop a peak at some incommensurate wave vector q_{inc} and, at the lowest c/a ratio, the susceptibility no longer attains its maximum value at $\mathbf{q} = \mathbf{0}$. This means that, rather than ordering ferromagnetically, the system will adopt an incommensurate antiferromagnetic structure, modulated along the c axis with the wave vector q_{inc}. **b**, Data for various unit cell volumes, using a c/a ratio of 1.54. The unit cell volumes are parameterized using Wigner–Seitz (W–S) radii, defined as the radius of a sphere of the same volume as the volume per atom. Atomic units (a.u.) are used, where 1 a.u. is the Bohr radius of a hydrogen atom. As the volume is increased, the height of the incommensurate peak relative to the $\mathbf{q} = \mathbf{0}$ (ferromagnetic) peak is reduced and at a W–S radius of 3.710 a.u. there is a near degeneracy between the two ordering types. For the highest W–S radii the ferromagnetic peak wins out. A similiar trend was observed for other, small, c/a ratios that correspond to systems having a webbing feature in their Fermi surface.
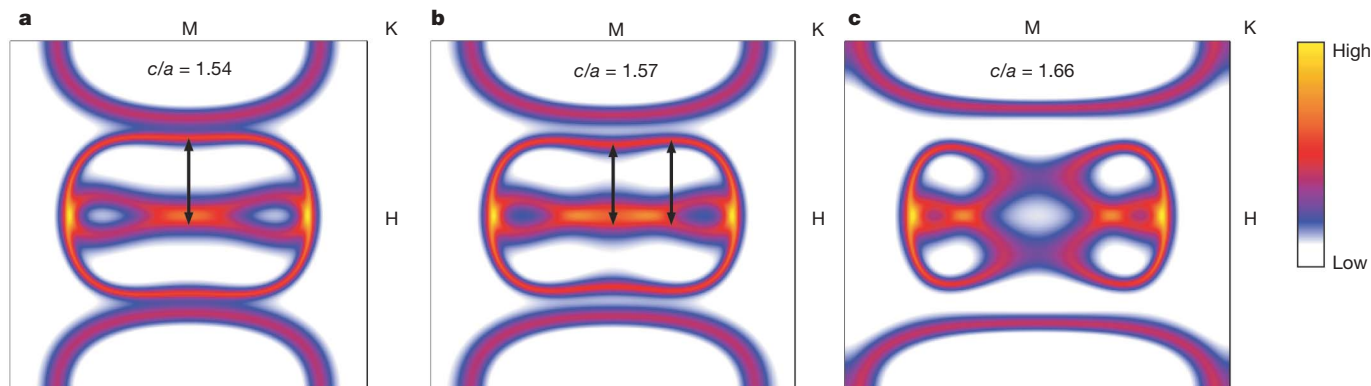
Figure 2 | Bloch spectral function of gadolinium on the HLMK plane of the hexagonal Brillouin zone, depicting the topology of the Fermi surface. The colour scale shows the spectral function in arbitrary units. Theoretical unit cell volumes were used, with the c/a ratios given in panels **a**, **b** and **c**. The centre of the plane is the L point. The Fermi surface in **a** has the 'webbing feature', with large sections of parallel Fermi surface that are separated by a nesting vector, indicated by the black arrow. The magnitude of the nesting vector is 0.2, which coincides with the size of the magnetic ordering wave vector q_{inc} that we obtained for this c/a ratio in Fig. 1a. As the c/a ratio increases, it is evident that the surfaces parallel to the KMK direction become less flat and at the highest c/a ratio the webbing structure is ruptured. This is concurrent with the transition to ferromagnetism observed in Fig. 1a.

Our key Fig. 3 summarizes the magnetic ordering tendencies of gadolinium as a function of c/a ratio and unit cell volume. Because $4f$ electrons are usually chemically inert, the heavy rare earth elements can all be considered as variations of the same entity and hence the behaviour of gadolinium as a function of lattice parameters is
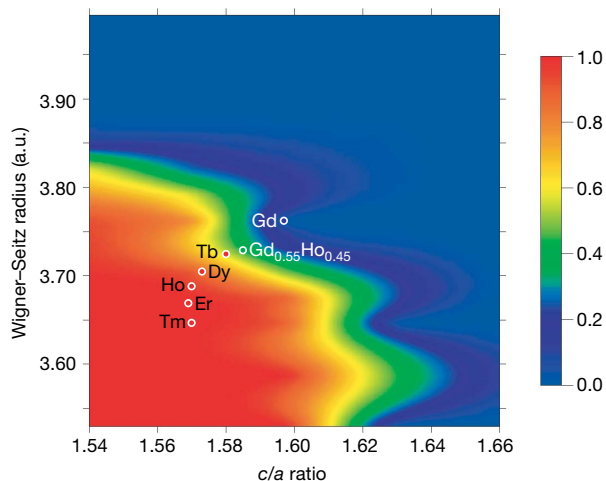

Figure 3 | Magnetic ordering tendencies of gadolinium (Gd) as a function of c/a ratio and W–S radii. On the colour scale, a value of 0 corresponds to when the paramagnetic state is dominated by ferromagnetic spin fluctuations, and a value of 1 corresponds to when it is dominated by spin fluctuations with some finite, incommensurate wave vector. For values between 0 and 1 the two ordering types compete: values below 0.5 indicate a stronger tendency towards ferromagnetic ordering and values above 0.5 indicate a greater tendency towards incommensurate antiferromagnetic ordering. A 3% shift was applied to the W–S radii, such that data shown at the experimental W–S radius of gadolinium corresponds to data calculated at the theoretical W–S radius of gadolinium. The experimental lattice parameters of all the heavy rare earth elements are indicated by circles: a blue (or red) circle indicates that experimentally the magnetic structure of the element is ferromagnetic (or incommensurate antiferromagnetic). The green circle indicates the experimental lattice parameters of a Gd–Ho alloy at the critical concentration of Ho at which an incommensurate antiferromagnetic phase first appears. From the phase diagram we predict the critical concentration of the $Gd_{1-x}Re_x$ alloys to be 0.78, 0.56, 0.49, 0.45, 0.42 for the heavy rare earth elements Tb (terbium), Dy (dysprosium), Ho (holmium), Er (erbium) and Tm (thulium) respectively. Experimental values are known only for dysprosium and holmium and are 0.50 (ref. 26) and 0.45 (ref. 27) respectively.

expected to mimic that of all the other heavy rare earth elements. Indeed, by examining where the experimental lattice parameters of all the heavy rare earth elements lie on Fig. 3, we predict that when going left to right in the heavy rare earth series there should be a trend away from ferromagnetism and towards incommensurate ordering. This is exactly what is observed experimentally, with the magnetic modulation vector starting out at zero for gadolinium (ferromagnetic ordering) and then progressively increasing through the series to produce various incommensurate antiferromagnetic structures.

From our ordering phase diagram (Fig. 3), we predict that the transition between ferromagnetism and incommensurate ordering occurs very rapidly as a function of c/a ratio, particularly for the higher unit cell volumes. This is consistent with recent experimental work on terbium, for which it was shown[25] that its incommensurately ordered phase could be completely suppressed by increasing the c/a ratio by as little as 0.002. In the phase diagram the elements dysprosium and terbium are positioned close to, or within, the transition region between ferromagnetic and incommensurate ordering. This concurs with the two systems' experimental behaviour, which exhibits incommensurate ordering at high temperatures and ferromagnetic ordering at low temperatures. Gadolinium is able to form alloys with all the heavy rare earth elements, with the alloys transforming from ferromagnets to incommensurate magnetically structured materials once the concentration of the heavy rare earth element exceeds a critical value. We used the phase diagram to predict these critical alloy concentrations and found them to be in good agreement with experimental values where known (see Fig. 3 legend).

We also computed estimates of the magnetic ordering vectors of all the heavy rare earth elements from our susceptibility calculations for gadolinium, the results of which are shown in Fig. 4, where the experimental trend is well reproduced. The magnetic ordering vectors of the last three members of the series (holmium, erbium and thulium) were found to lie very close together, in agreement with experiment. Owing to its half-filled $4f$ shell, the gadolinium ion has orbital angular momentum $L = 0$. Hence the effects of spin orbit coupling can be neglected in our calculations of gadolinium. For the other heavy rare earth elements, however, the coupling of spin and orbital moments is important in obtaining estimates of their magnetic moments and magnetic ordering temperatures. Indeed, by accounting for this aspect, we used the gadolinium results to reproduce trends in magnetic ordering temperatures, as shown in the inset of Fig. 4. Nonetheless, the type of magnetic order and magnetic ordering vector are determined by the spd conduction electrons, which are little affected by spin-orbit coupling and which all the heavy rare earths have in common.
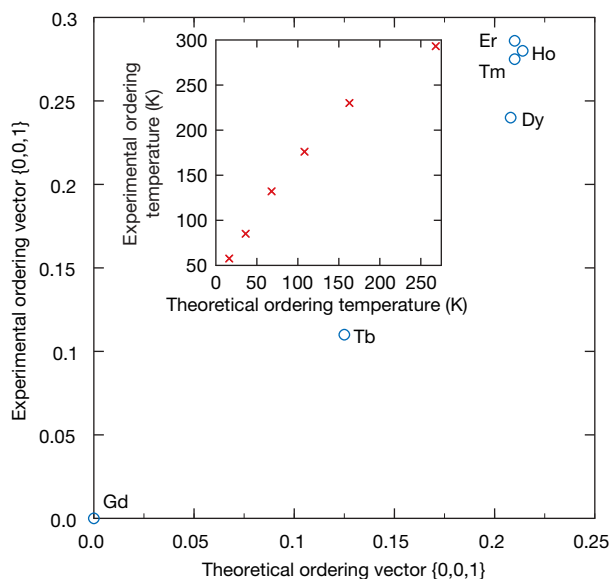
Figure 4 | Experimental magnetic ordering vectors of the heavy rare earth elements versus those predicted from *ab initio* calculations for gadolinium. The ordering vectors are obtained by performing susceptibility calculations for gadolinium at the appropriate lattice parameters. For example, when we performed a calculation at the experimental lattice parameters of terbium the susceptibility peaked at a wave vector $\mathbf{q} = \{0, 0, 0.13\}$, in good agreement with the experimental ordering vector, $\{0, 0, 0.11\}$. The inset shows the corresponding ordering temperatures. Experimentally, gadolinium has the highest ordering temperature, which decreases monotonically through the heavy rare earth series. To take into account the different total angular momentum values J of the heavy rare earth elements, the theoretical ordering temperatures have been scaled according to the de Gennes factor[28] $(g_J - 1)^2 J(J + 1)$, where g_J is the Lande g-factor. It is clear that the results from the gadolinium study reproduce the experimental trend, although the magnitudes of the temperatures are systematically underestimated.

The parts that the different types of valence electrons play in determining the magnetic structures of the heavy rare earth elements are thus clear; the itinerant *spd* electrons, common to all the heavy rare earth elements, mediate the interaction between magnetic moments and it is the nesting of their Fermi surfaces which can lead to instabilities in the paramagnetic phase with respect to the formation of incommensurate spin density waves. The *f* electrons, on the other hand, are responsible for setting up the magnetic moments and, as their number increases across the heavy rare earth series, they play an indirect role in promoting incommensurate order by shrinking the unit cell volume through the lanthanide contraction.

1. Gschneidner, K. A. & Eyring, L. (eds) *Handbook on the Physics and Chemistry of Rare Earths* Vol. 1 (North Holland, Amsterdam, 1978).
2. Jensen, J. & Mackintosh, A. K. *Rare Earth Magnetism* 286–304 (Clarendon, Oxford, 1991).
3. Keeton, S. C. & Loucks, T. L. Electronic structure of rare-earth metals. I. Relativistic augmented-plane-wave calculations. *Phys. Rev.* **168**, 672–678 (1968).
4. Fretwell, H. M. *et al.* Fermi surface as the driving mechanism for helical antiferromagnetic ordering in Gd-Y alloys. *Phys. Rev. Lett.* **82**, 3867–3870 (1999).
5. Cracknell, A. P. & Wong, K. C. *The Fermi Surface* (Clarendon, Oxford, 1973).
6. Taylor, K. N. R. & Darby, M. I. *Physics of Rare Earth Solids* 60–62 (Chapman and Hall, London, 1972).
7. Hubbard, J. Magnetism of iron. II. *Phys. Rev. B* **20**, 4584–4595 (1979).
8. Gyorffy, B. L., Pindor, A. J., Staunton, J., Stocks, G. M. & Winter, H. A first-principles theory of ferromagnetic phase transitions in metals. *J. Phys. F* **15**, 1337–1386 (1985).
9. Heinemann, M. & Temmerman, W. M. Magnetic structures of hcp bulk gadolinium. *Phys. Rev. B* **49**, 4348–4351 (1994).
10. Kurz, P., Bihlmayer, G. & Blügel, S. Magnetism and electronic structure of hcp Gd and the Gd(0001) surface. *J. Phys. Condens. Matter* **14**, 6353–6371 (2002).
11. Eriksson, O. *et al.* Bulk and surface magnetism and interplanar spacings in Gd from first-principles calculations. *Phys. Rev. B* **52**, 4420–4426 (1995).
12. Harmon, B. N., Antropov, V. P., Liechtenstein, A. I., Solovyev, I. V. & Anisimov, V. I. Calculation of magneto-optical properties for 4f systems: LSDA + Hubbard U results. *J. Phys. Chem. Solids* **56**, 1521–1524 (1994).
13. Perdew, J. P. & Zunger, A. Self-interaction correction to density-functional approximations for many-electron systems. *Phys. Rev. B* **23**, 5048–5079 (1981).
14. Strange, P., Svane, A., Temmerman, W. M., Szotek, Z. & Winter, H. Understanding the valency of rare earths from first-principles theory. *Nature* **399**, 756–758 (1999).
15. Lüders, M. *et al.* Self-interaction correction in multiple scattering theory. *Phys. Rev. B* **71**, 205109 (2005).
16. Rado, G. T. & Suhl, H. (eds) *Magnetism* Vol. IIB 337–377 (Academic Press, New York, 1966).
17. Staunton, J. B. & Gyorffy, B. L. Onsager cavity fields in itinerant-electron paramagnets. *Phys. Rev. Lett.* **69**, 371–374 (1992).
18. Turek, I., Kudrnovský, J., Bihlmayer, G. & Blügel, S. *Ab initio* theory of exchange interactions and the Curie temperature of bulk Gd. *J. Phys. Condens. Matter* **15**, 2771–2782 (2003).
19. Andrianov, A. V. Helical magnetic structures in heavy rare-earth metals as a probable manifestation of the electronic topological transition. *J. Magn. Magn. Mater.* **140–144**, 749–750 (1995).
20. Lifshitz, I. M. Anomalies of electron characteristics of a metal in the high pressure region. *Sov. Phys. JETP* **11**, 1130–1135 (1960).
21. Blanter, Y. M., Kaganov, M. I., Pantsulaya, A. V. & Varlamov, A. A. The theory of electronic topological transitions. *Phys. Rep.* **245**, 159–257 (1994).
22. Evenson, W. E. & Liu, S. H. Generalized susceptibilities and magnetic ordering of heavy rare earths. *Phys. Rev.* **21**, 432–434 (1968).
23. Dugdale, S. B. *et al.* Direct observation and calipering of the "webbing" Fermi surface of yttrium. *Phys. Rev. Lett.* **79**, 941–944 (1997).
24. Nordström, L. & Mavromaras, A. Magnetic ordering of the heavy rare earths. *Europhys. Lett.* **49**, 775–781 (2000).
25. Andrianov, A. V., Kosarev, D. I. & Beskrovnyi, A. I. Helical magnetic ordering in Tb completely suppressed by uniaxial tension: Evidence of electronic topological transition and support for the nesting hypothesis. *Phys. Rev. B* **62**, 13844–13847 (2000).
26. Milstein, F. & Robinson, L. B. Magnetic transitions in alloys of gadolinium and dysprosium. *Phys. Rev.* **159**, 466–472 (1967).
27. Andrianov, A. V. & Chistiakov, O. D. Evidence of pressure-induced antiferromagnetism in ferromagnetic $Ho_{0.4}Gd_{0.6}$. *Phys. Rev. B* **55**, 14107–14108 (1997).
28. Blundell, S. *Magnetism in Condensed Matter* 91–92 (Oxford Univ. Press, Oxford, 2001).

Author Information Reprints and permissions information is available at www.nature.com/reprints. The authors declare no competing financial interests. Correspondence and requests for materials should be addressed to I.D.H. (i.d.hughes@warwick.ac.uk) or J.B.S. (j.b.staunton@warwick.ac.uk).